MODELLING OF TRIAXIAL WOVEN FABRICS FOR ANTENNA REFLECTORS

Andreas Obst, Giuseppe Palermo, Lorenzo Ticci, Julian Santiago Prowald

European Space Agency, TEC-MCS, Keplerlaan 1, 2201 AZ Noordwijk, The Netherlands

ABSTRACT

In this paper the status of on-going work on the modelling of Triaxial Woven Fabrics (TWF) is presented. Some conclusions are drawn and necessary further steps are outlined.

In order to achieve severe requirements for areal weight of advanced antenna reflectors TWF are introduced in the reflector shell design. Triaxial woven fabrics are composed of three sets of carbon fiber yarns that interlace at 0°, –60° and +60° degrees with small holes in between the yarns. The TWF offer a very good stiffness-to-mass ratio and good dynamic behaviour for low as well as high frequency domain.

However, the thermo-mechanical behavior of the TWF is complex due to the strong influence of geometrical parameters and therefore difficult to analyze. TWF can exhibit significant out-of-plane deformation under in-plane mechanical or under thermal loads. Different approaches to model the thermo-mechanical behavior of TWF were reviewed and finite element models of different complexity developed. The study showed that while rather simple models yield adequate results for the prediction of the in-plane elastic constants, these models fail to capture the out-of-plane deformations due to mechanical or thermal loading.

As a consequence detailed 3D finite element models were developed that take into account all geometrical parameters of the yarn. The intention was to use these models as a benchmark to evaluate the performance of more simple models. Initial results showed good agreements with literature test data. However, later results with a refined 3D model were different and put the initial results in question. Nevertheless, the models demonstrate the complex behaviour of TWF and also the strong influence of boundary conditions on the results.

The 3D model was used to predict engineering constants for TWF and to study the deformations of coupons under mechanical or thermal loads, i.e., to simulate coupon testing. The analyses demonstrate that care has to be taken in the designing of coupon tests for thermo-mechanical characterization of TWF. A significant variation of properties with coupon size and applied "test" boundary conditions can be seen.

Finally, an attempt was made to use a homogenisation procedure to derive an equivalent ABD matrix for TWF.

1. INTRODUCTION

Due to their excellent stiffness-to-mass ratio, triaxial woven fabrics find application in communication satellite reflectors. TWF were subject of several previous and on-going ESA studies.

Advantages of TWF are:

- Extreme light weight (< 1 kg/m^2).
- Very high stiffness-to-mass ratio.
- Open hole structure rendering acoustic load cases almost irrelevant.

A schematic of the interlacing yarns of TWF and a reflector developed in an ESA study are shown in Figure 1 and Figure 2, respectively.

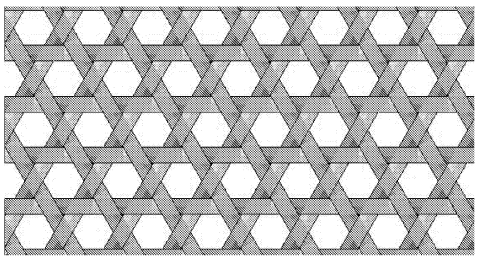

Figure 1: Schematic of triaxial woven fabric

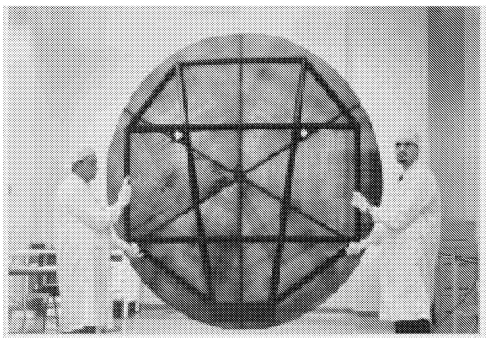

Figure 2: ASRA-B CFRP ultra-light 2.2-m shaped reflector EQM (Alenia Spazio) [1]

European Conference on Spacecraft Structures, Materials & Mechanical Testing 2005
Noordwijk, The Netherlands, 10 – 12 May 2005 (ESA SP-581, August 2005)

A major challenge in the application of TWF, particularly of single layer TWF, is in the modelling to predict the mechanical and thermal performance of the structure. This is due to the complex geometry of interlacing yarns and the resulting complex mechanical behaviour:

- With yarns interlacing at 0°, –60° and +60° degrees an isotropic in-plane behaviour could be expected, however, test and analysis results show that this is not the case.
- TWF exhibit strong couplings (stretch-twist, bend-twist, …).
- Equivalent mechanical properties depend on specimen size and "test" boundary conditions.

As a consequence, complex analytical or FEM models are needed to capture all effects. Detailed FEM models need to adequately represent the behaviour of a unit cell of the TWF. However, such models are too detailed to be applied to full reflector structures and some simplified models or homogenized properties have to be derived.

While correlation between FEM results and measured mechanical properties is usually good, correlation to thermo-elastic measurements is difficult.

The objectives of the present study were to:

- review the state-of-the-art in modelling of TWF,
- develop a detailed benchmark FEM model based on a unit cell approach in which the geometry is accurately represented,
- use 3D FEM with solid elements to capture out-of-plane effects, and
- develop a homogenization approach to derive equivalent laminate properties from the complex model.

2. TWF MODELLING APPROACHES

Models of various degrees of complexity are used for the modelling of TWF. These range from simple laminate models to detailed FEM for TWF unit cells. Different beam and shell FEM were compared to some experimental data by Schrama [2]. Hoa published a series of papers [3-6] in which different models for TWF are developed and compared to test results. These models are described in some more detail in the following.

2.1 Laminate Models

Laminate models are the most simple models for TWF. Here the TWF is modelled as a laminate of the same total thickness and composed of 3, 6 or more uni-directional layers (Figure 3) that are oriented at -60°, 0° and 60°. The uni-directional ply properties are determined by scaling the yarn properties by the ratio of the actual cross-sectional area for each direction in the TWF to the cross-sectional area in the laminate model. In case a 3 layer model results in too strong coupling terms compared to the real TWF more than 3 layers are used to "adjust" these couplings.

The main advantages of laminate models are their simplicity and that they can be easily be used for large structure modelling. Disadvantages are that they do not capture through-thickness effects, do not represent all couplings accurately and in contrast to measured data are fully isotropic in the plane of the laminate.

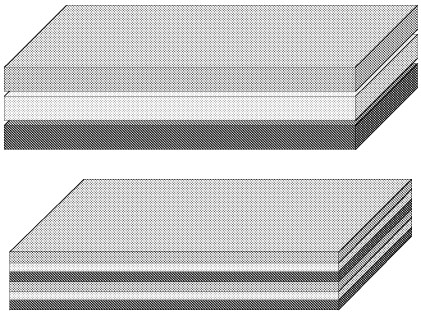

Figure 3: Laminate models for TWF

2.2 Variational Potential Energy Method

An equivalent energy approach to predict the properties of TWF was developed by Hoa [3]. In this approach the 3D geometry of the TWF is accurately taken into account. The principle of minimum potential energy with the iso-strain assumption and the principle of minimum complementary energy with the iso-stress assumption are used to predict upper and lower bounds of the TWF elastic constants, respectively.

2.3 Beam and Shell Finite Element Models

Several beam and shell finite element models for unit cells of TWF were studied by Schrama [2]. These models represent the 3D geometry of a TWF unit cell. The unit cell model was then "multiplied" to model test coupons. Analysis results were compared to some available test results. Good predictions of TWF elastic constants could be achieved, but prediction of coefficients of thermal expansion (CTE) was not as good. The shell models were superior to the beam models.

2.4 Superelement Models

Special finite element models (superelements) for TWF unit cells were developed by Zhao and Hoa and used to predict elastic constants and CTE of TWF [4-6]. To develop the superelements the unit cell was split into several parts (Figure 4) and for each part a finite element representation was developed. The parts were assembled using a pseudo-element technique and then internal nodes were eliminated to obtain the final superelement. Two superelements were developed: one in which yarn cross-over locations are connected by straight sections and one in which the twisting of the yarns is accurately represented. The latter is more complicated but gives better results.

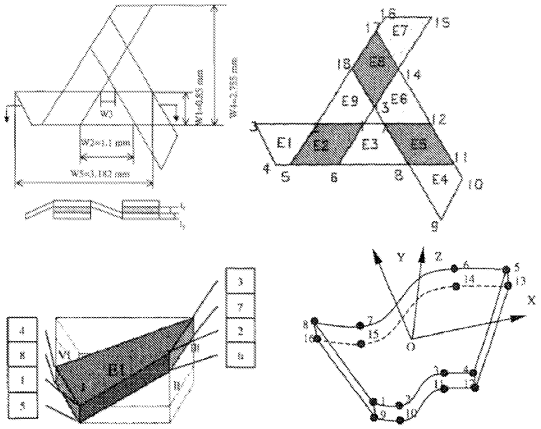

Figure 4: Representation of unit cell in superelement development (Zhao [4])

2.5 Literature Data

In this section some data, analysis and test results for TWF found in literature are presented (Zhao [4-6]). For the development of the full 3D finite element models the same geometrical parameters for the TWF unit cell as shown by Zhao were used. This literature data was also used to check the predictions with the detailed model.

Geometrical parameters are indicated in Figure 4. Yarn elastic properties are shown in Table 1.

Table 1: Yarn properties [4]

E_1 [GPa]	E_2 [GPa]	G_{12} [GPa]	ν_{12}	ν_{23}
338.57	12.4	5.61	0.287	0.437

In Table 2 test results presented by Zhao are compared to predictions with some of the models discussed.

Table 2: Test and analysis results for TWF (Zhao [3-5])

Model	E_1 [GPa]	E_2 [GPa]	ν_{12}
Experiment	32.24	20.5	0.55
Standard deviation	5.63	2.54	
Energy upper bound	37.3	36.5	0.303
Energy lower bound	20.8	20.8	0.274
SE1	36.88	33.61	0.51
SE2	30.01	26.55	0.58

3. DETAILED 3D FEM MODEL

In the present study detailed 3D FE models were developed for TWF unit cells. These unit cells were then replicated to obtain larger models. In the first 3D FEM the undulating parts of the yarns between the crossing regions were approximated by straight sections. In a refined model sine functions were used for the undulating parts to also account for the twisting of the yarns. The entire model of a unit cell was meshed using hexagonal solid elements. Mesh density was varied to check for convergence of the models. It was found that two elements through the thickness and across the width of a yarn give converged results.

Solid elements were used for the yarns to be able to account for eventual through-thickness expansion effects of the yarn on predicted thermo-elastic deformations and apparent CTE. Shell elements do not account for any through-thickness deformation.

In Figure 5 a FEM of a TWF unit cell is shown. In this model the cross-over regions were connected with straight yarn sections. The unit cell geometry was the same as proposed by Zhao. If such a unit cell is replicated to model a larger TWF part, the boundaries are rather ragged. To simplify the application of boundary conditions a different unit cell was selected (see also Figure 5). Parts modelled with such a new unit cell have smoother boundaries and it is simpler to apply boundary conditions. Analysis performed with both unit cells showed that the type of unit cell had negligible influence on the results.

In the initial models the material orientation was not fully aligned with the yarn orientation at the undulating parts. The in-plane orientations were correct but the material coordinate system remained in the plane of the fabric and did not follow the slopes of the yarns in the undulating regions. Due to the small slopes this was thought to be a reasonable approximation. In the later

models this was corrected and the material orientation was adjusted for each solid element individually.

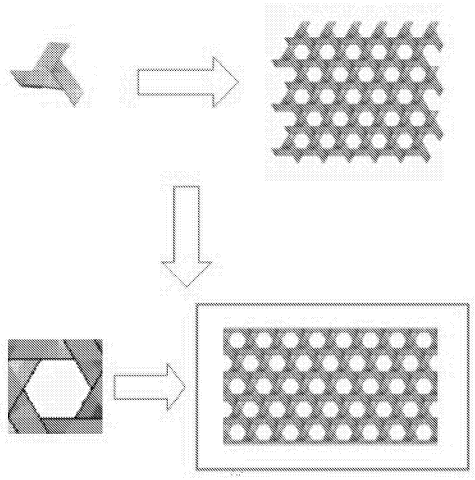

Figure 5: Different unit cells for TWF

As was shown by Zhao [5] and in Table 2, the twisting of the yarns between the cross-over regions can have an influence on predicted apparent mechanical properties. Therefore also a refined model that accounts for the twisting of the yarns was developed. A section of such a model is shown in Figure 6.

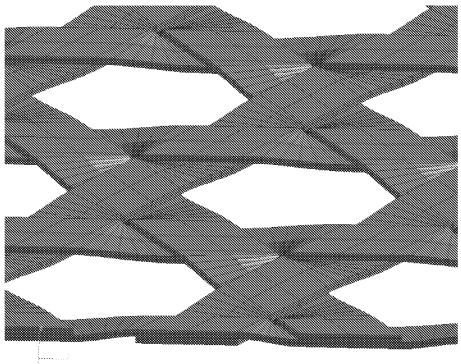

Figure 6: Refined FEM of TWF

4. PREDICTION OF APPARENT THERMO-MECHANICAL PROPERTIES OF TWF

To verify the developed 3D FEM mechanical properties of TWF were calculated. In order to determine the apparent E-moduli in x- and y-direction "test" coupons were modelled (Figure 7). A uni-directional tension test was simulated by applying a uniform displacement at one end while fixing the other end. The apparent E-modulus can then be calculated using the equation

$$E = \frac{F \cdot L}{w \cdot H \cdot d}$$

where F is the force resultant at the fixed end, d is the applied displacement, L and w are the length and width of the test section, respectively, and H is the thickness of the laminate.

To study the influence of the "test coupon size" on the E-modulus prediction different aspect ratios were analysed. The results are shown in Table 3. As can be seen the results converge with increasing length to width ratio of the coupons. Also agreement with literature results appeared good.

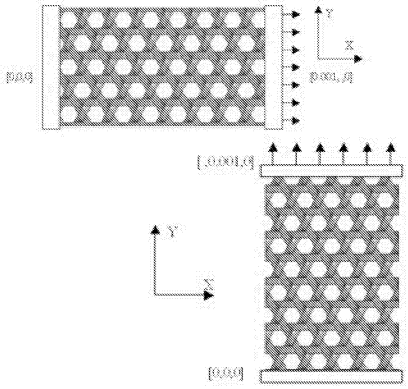

Figure 7: Test coupon models for E-modulus prediction

Table 3: Predicted apparent E-moduli of TWF

Aspect ratio	0.923	1.85	3	3.93
E_x [GPa]	30.1	28.8	28	28
Aspect ratio	0.867	1.73	2.77	3.47
E_y [GPa]	27.9	25.9	25.5	25.4

As illustrated in Figure 8, in small size "coupons" the number of off-axis yarns that are clamped between the supports is larger than in larger specimens. In fact, most of the yarns in a larger specimen are not clamped at all. If a yarn is clamped at a support its rotation is restricted. This explains that the E-modulus for a small coupon is larger than for large coupons.

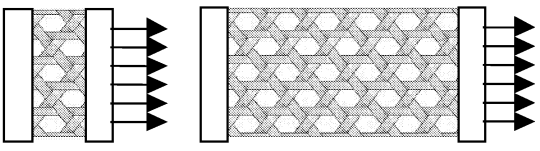

Figure 8: Clamped yarns in different size specimens

The deformation of the TWF under applied uniform displacement in x-direction is shown in Figure 9. This clearly shows the complex deformation pattern. It also illustrates that even under simple in-plane load

conditions significant out-of-plane displacements can occur.

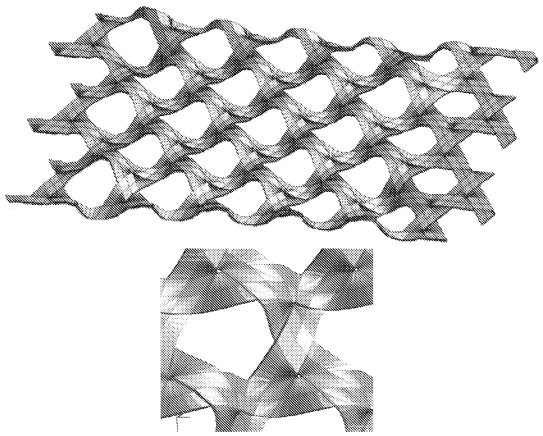

Figure 9: Deformation of TWF under applied uniform axial displacemment

To predict the apparent shear modulus of TWF a rail shear test was simulated. As shown in Figure 10, two different orientations of the TWF in the "fixture" were considered. In one case the longitudinal yarns were parallel to the moving clamp direction, in the other case they were perpendicular. Again different aspect ratios were considered. The calculated apparent shear moduli for both directions are shown in Table 4. The results show some dependence on the aspect ratio. Interestingly, also the orientation of the specimen had an influence on the calculated modulus. This most likely can be attributed to the different number of clamped yarns in the two cases and illustrates the difficulty even in interpreting test data for this material.

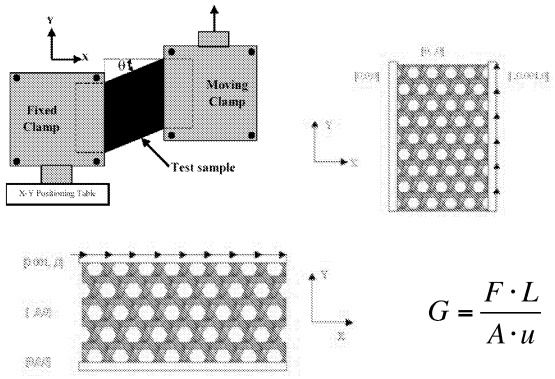

$$G = \frac{F \cdot L}{A \cdot u}$$

Figure 10: Simulation of rail shear test for apparent shear modulus prediction

Table 4: Predicted apparent shear modulus of TWF

Aspect ratio	0.923	1.85	3	3.93
G_1 [GPa]	19.7	19.6	19.6	19.6
Aspect ratio	0.867	1.73	2.77	3.47
G_2 [GPa]	15.2	16.5	17.1	17.2

To calculate the apparent CTE of the TWF iso-statically fixed models with different aspect ratios were analysed. The models, boundary conditions and resulting deformations are shown in Figure 11. A strong influence of the boundary conditions on the deformation pattern can be observed. If two yarns with opposite slopes at the supported end are fixed, then the resulting deformation is predominately twisting. When yarns with equal slopes are fixed then out-of-plane bending is predominant. Also, in either case the free end of the specimen did not deform uniformly. Therefore it was difficult to determine the in-plane displacement that should be used to calculate the apparent CTE. Results obtained by using the average displacement at the free end are shown in Table 5. A very strong influence of the aspect ratio can be seen. The cause of this is not fully understood but could have to do with the additional bending and twisting of the specimen.

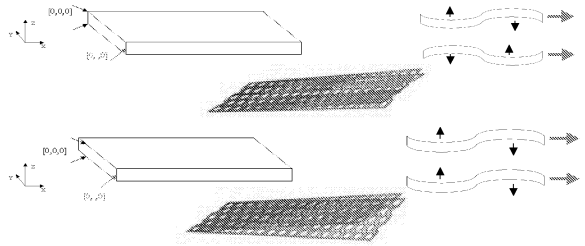

Figure 11: Models for apparent CTE prediction

Table 5: Predicted apparent CTE of TWF

Aspect ratio	0.923	1.85	3	3.93
α_x [10^{-6}/°C]	2.42	1.47	1.11	0.969

As mentioned before, in the initial models the material orientation at the undulating regions was only approximated. In the refined models the material orientation was correctly modelled for all elements and twisting of the yarns between crossing points was represented. It was expected that accounting for the twisting would result into a slightly lower predicted apparent E-modulus, similar to the observations of Zhao (see results in Table 2). However, the predicted modulus was only about half of that obtained with the previous model. At the time of this writing work is ongoing to try to understand this difference and no conclusions on this aspect can be presented.

5. DERIVATION OF HOMOGENIZED TWF PROPERTIES

Since the detailed 3D FEM is not suitable for modelling entire antenna reflectors an attempt was made to calculate equivalent homogenized properties for TWF that could then be assigned to simple shell element models of a reflector. In this approach an equivalent ABD matrix is derived for the TWF by applying unitary self-balancing loads to a model of the fabric. As shown

below each unitary load case gives one column of the equivalent laminate compliance matrix. This matrix can then be inverted to obtain the equivalent ABD matrix for the TWF.

The laminate stiffness matrix is:

$$\begin{Bmatrix} N_x \\ N_y \\ N_{xy} \\ M_x \\ M_y \\ M_{xy} \end{Bmatrix} = \begin{bmatrix} A & B \\ B & D \end{bmatrix} \begin{Bmatrix} \varepsilon_x \\ \varepsilon_y \\ \varepsilon_{xy} \\ K_x \\ K_y \\ K_{xy} \end{Bmatrix}$$

Expanding and inverting this matrix results in:

$$\begin{aligned}
\varepsilon_x &= a_{11}N_x + a_{12}N_y + a_{16}N_{xy} + b_{11}M_x + b_{12}M_y + b_{16}M_{xy} \\
\varepsilon_y &= a_{12}N_x + a_{22}N_y + a_{26}N_{xy} + b_{12}M_x + b_{22}M_y + b_{26}M_{xy} \\
\varepsilon_{xy} &= a_{16}N_x + a_{26}N_y + a_{66}N_{xy} + b_{16}M_x + b_{26}M_y + b_{66}M_{xy} \\
K_x &= b_{11}N_x + b_{12}N_y + b_{16}N_{xy} + d_{11}M_x + d_{12}M_y + d_{16}M_{xy} \\
K_y &= b_{12}N_x + b_{22}N_y + b_{26}N_{xy} + d_{12}M_x + d_{22}M_y + d_{26}M_{xy} \\
K_{xy} &= b_{16}N_x + b_{26}N_y + b_{66}N_{xy} + d_{16}M_x + d_{26}M_y + d_{66}M_{xy}
\end{aligned}$$

If unitary self-balancing loads are applied only one term of the right hand side of each row is non-zero. These are shown for applied N_x and N_y below.

$$\begin{aligned}
\varepsilon_x &= a_{11}N_x = a_{11} & \varepsilon_x &= a_{12}N_y = a_{12} \\
\varepsilon_y &= a_{12}N_x = a_{12} & \varepsilon_y &= a_{22}N_y = a_{22} \\
\varepsilon_{xy} &= a_{16}N_x = a_{16} & \varepsilon_{xy} &= a_{26}N_y = a_{26} \\
K_x &= b_{11}N_x = b_{11} & K_x &= b_{12}N_y = b_{12} \\
K_y &= b_{12}N_x = b_{12} & K_y &= b_{22}N_y = b_{22} \\
K_{xy} &= b_{16}N_x = b_{16} & K_{xy} &= b_{26}N_y = b_{26}
\end{aligned} \quad \ldots$$

The results can be organized schematically as:

	N_x	N_y	N_{xy}	M_x	M_y	M_{xy}
ε_x	a_{11}	a_{12}	a_{16}	b_{11}	b_{12}	b_{16}
ε_y	a_{12}	a_{22}	a_{26}	b_{12}	b_{22}	b_{26}
γ_{xy}	a_{16}	a_{26}	a_{66}	b_{16}	b_{26}	b_{66}
κ_x	b_{11}	b_{12}	b_{16}	d_{11}	d_{12}	d_{16}
κ_y	b_{12}	b_{22}	b_{26}	d_{12}	d_{22}	d_{26}
κ_{xy}	b_{16}	b_{26}	b_{66}	d_{16}	d_{26}	d_{66}

By inversion of this matrix the equivalent laminate stiffnees matrix (ABD-matrix) is obtained.

To be able to use this approach a method to extract the strain and curvatures from the results for each applied load case is needed. One approach to obtain these could be to fit a surface to deformed laminates and extract the strains and curvatures from these surfaces. In the present study a simpler approach was chosen. In that approach a dummy shell element is connected to the mid-surface of the solid element mesh. Care has to be taken that the correct rotations are transferred from the deformed solid element mesh to the dummy shell element. When the loads are applied the solid element model deforms and the dummy shell element deformation reflects the average deformation of the model. The strains and curvatures for the dummy shell element can then directly be extracted from finite element results file.

The approach was verified by modeling a multiple layer unsymmetric and unbalanced laminate, for which all coefficients of the ABD matrix are non-zero, with solid elements for each layer. The ABD matrix calculated using the described approach was identical to that calculated using laminate theory. In a second verification the equivalent ABD matrix for a plain weave fabric that was modeled in detail with solid elements was calculated.

When applying this approach to the TWF FE model some difficulties were encountered. Due to the open hole structure and the non-smooth boundaries of the TWF it was difficult to apply self-balancing unitary loads to the edges. Due to the significantly varying local stiffness of the TWF between an edge at cross-over regions and single yarn regions even a uniform applied load on this edge resulted in some local deformation and not a smooth transfer of the loads to the entire laminate. Also connecting the dummy shell element to the model proved difficult since connection to parts with low local stiffness (single yarn parts) should be avoided.

The TWF FEM and resulting deformations under the applied load cases are shown in Figure 12.

The calculated ABD matrix is:

5798	2977	-.026	4.47E-4	2.60E-4	-2.260
3472	5554	-.027	1.06E-3	4.80E-4	1.879
-.0128	-5.58E-3	1271	-4.603	-.918	-1.87E-4
4.99E-4	8.67E-4	1.311	3.917	.959	3.60E-6
1.80E-4	7.16E-4	.822	1.042	3.794	8.35E-6
-7.581	-4.940	-6.37E-6	4.81E-6	2.03E-5	1.367

Calculating A_{11} and A_{22} from the predicted equivalent properties in Table 3 and the Poisson ratio for superelement 2 from Table 2, results in A_{11} = 5369 N/mm and A_{22} = 4848 N/mm. Considering that the boundary conditions are different to the case analyzed for determining the equivalent properties and that the Poisson ratio has been taken from another model, the agreement for these terms with the ABD matrix calculated using the homogenization approach is good.

However, looking a the off-axis terms in the calculated ABD matrix, it is apparent, that there are some problems in the predictions because the matrix is not symmetric. The cause of this can most likely be attributed to the non-perfect load introduction for the

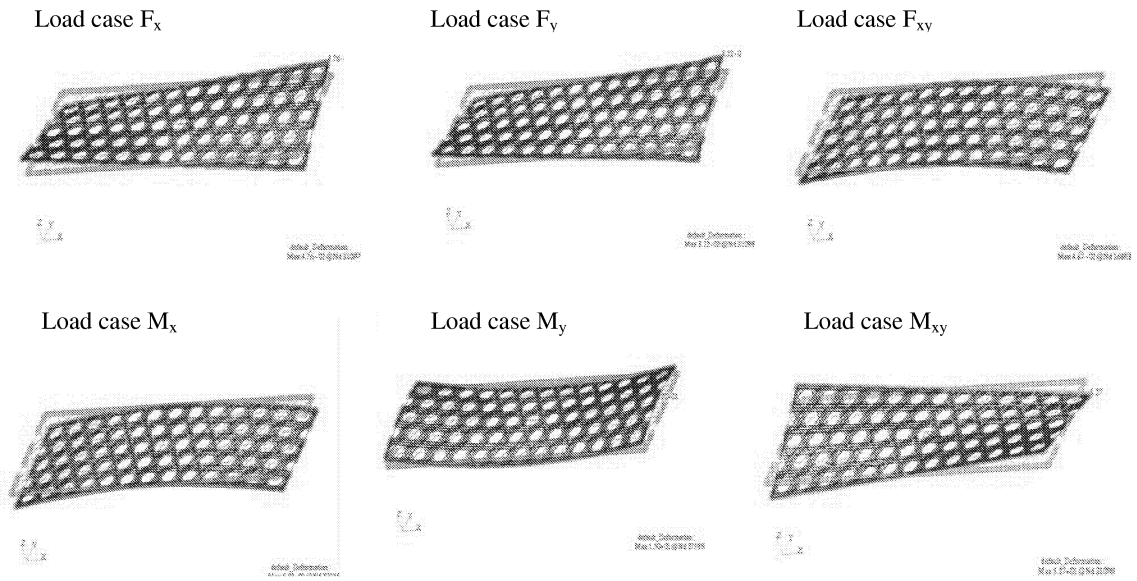

Figure 12: Deformation resulting from applied unitary load cases

unitary load cases and the connection of the dummy shell element to the solid element model. The out-of-plane deformations are larger at the edges of the model than at the center and therefore the strains and curvatures extracted from the dummy element depend on the location where the dummy element is fixed. At the time of this writing work is in progress to further analyze this and also to find a different method for reducing the size of the detailed 3D models.

6. CONCLUSIONS

Detailed 3D finite element models for the analysis of TWF were developed. The analyses performed using these models demonstrate the complex behaviour of this type of fabric. Small changes in modelling assumptions, load introduction and boundary conditions can have a significant influence on the predictions. In a next step the models will be correlated with new test results on TWF which then should validate the modelling approach. The models can then be used as benchmark to evaluate simplified models.

The applied homogenisation procedures produced an unsymmetric apparent ABD matrix. This was thought to be due to the non-perfect load application on the edges of the analysed "specimens". Due to the non-smooth edges of the TWF it appears not possible to better apply the loads to the boundaries. Therefore, other methods to obtain homogenized properties or to reduce the model size are under investigation.

7. REFERENCES

1. C. Bruno, et al. (1998), "ASRA-B - An Advanced Shaped Reflector Antenna," Preparing for the Future Vol. 8 No. 2, European Space Agency Publication.

2. M.S. Schrama (1993), "Determining the properties of a triaxial woven single ply carbon fiber fabric with the aid of FEM analysis," *ESA/ESTEC TEC/MCS Internal Report.*

3. S.V. Hoa, S.Z. Sheng and P. Ouellette (2003), "Determination of elastic properties of triax composite materials," *Composites Science and Technology, Vol. 63, pp. 437–443*

4. Q. Zhao and S.V. Hoa (2003), "Triaxial Woven Fabric (TWF) Composites with Open Holes (Part I): Finite Element Models for Analysis," *Journal of Composite Materials, Vol. 37, No. 9, pp. 763-789.*

5. Q. Zhao, S.V. Hoa and P. Ouellette (2003), "Triaxial Woven Fabric (TWF)Composites with Open Holes (Part II): Verification of The Finite Element Models," *Journal of Composite Materials, Vol. 37, No. 10, pp. 849-873*

6. Q. Zhao and S.V. Hoa (2003), "Thermal Deformation Behavior of Triaxial Woven Fabric (TWF) Composites with Open Holes," *Journal of Composite Materials, Vol. 37, No. 18, pp. 1629-1649.*